Ocean Dynamics (2016) 66:195–206
DOI 10.1007/s10236-016-0923-5

The influence of Black Sea Water inflow and its synoptic time-scale variability in the North Aegean Sea hydrodynamics

Apostolia-Maria Mavropoulou[1] · **Anneta Mantziafou**[1] · **Ewa Jarosz**[2] · **Sarantis Sofianos**[1]

Received: 29 July 2015 / Accepted: 12 January 2016 / Published online: 4 February 2016

Abstract The exchange water fluxes between the Black Sea and the North Aegean Sea through the Dardanelles Strait constitute an essential factor for the general circulation of the region. The Black Sea Water (BSW) inflow to the Aegean plays an important role in the hydrography and circulation of the basin and can affect the North Aegean deep water formation processes. Numerical experiments evaluating the influence of the time-scale variability (synoptic and seasonal) and the seasonality (period of maximum/minimum) of the Black Sea Water inflow on the dynamics of the North Aegean basin were performed. The experiments were carried out for the period from August 2008 to October 2009, using observed upper and lower-layer fluxes from the Dardanelles Strait, high-resolution atmospheric forcing, and boundary conditions derived from an operational system (ALERMO). The large-scale spatial patterns of the circulation and the seasonal variability of the North Aegean circulation show that dynamics of the basin can effectively absorb most of the Black Sea Water inflow variability. The overall cyclonic circulation of the North Aegean Sea and the predominant cyclonic and anti-cyclonic features are robust and are little affected by the different lateral fluxes. However, differences in the seasonality of the BSW inflow have an important impact in the North Aegean water column structure, while the synoptic variability observed in the Black Sea Water inflow affects the kinetic energy of the basin and the pathway of the Black Sea Water plume.

Keywords North Aegean · Black Sea Water · Observed data · Numerical modeling · Ocean circulation

Responsible Editor: Emil Vassilev Stanev

✉ Apostolia-Maria Mavropoulou
mmavro@oc.phys.uoa.gr

[1] Division of Environmental Physics, University of Athens, Athens, Greece

[2] Naval Research Laboratory, Stennis Space Center, Mississippi, USA

1 Introduction

The North Aegean (Fig. 1) is a semi-enclosed basin that occupies the northeastern part of the Eastern Mediterranean Sea, between the Greek peninsula and Turkey. The North Aegean basin is characterized by complicated bottom topography and has a large number of islands, gulfs, deep and shallow depressions. It constitutes a link between the Mediterranean Sea and the Black Sea as the Black Sea Water (BSW) reaches the Aegean Sea through the Turkish Strait System (TSS), which includes the Bosphorus Strait, the Marmara Sea and the Dardanelles Strait. The TSS connects two adjacent basins with significant salinity and density differences, and the exchange flow is characterized by a two-layer structure. In the Dardanelles Strait, the upper layer is occupied by brackish waters originating from the Black Sea and flowing towards the North Aegean Sea and the lower layer contains salty waters from the Aegean Sea, which move approximately northeastward towards the Marmara Sea (Ünlüata et al. 1990; Tuğrul et al. 2002; Jarosz et al. 2012).

The BSW spread in the North Aegean and the extent of its influence on the circulation is related to its volume inflow rate in the Dardanelles Strait (Tzali et al. 2010). The exchange rate in the Dardanelles Strait has been estimated in several studies that use either in situ observations (Ünlüata et al. 1990; Latif et al. 1991; Beşiktepe et al. 1994; Jarosz et al. 2013) or parameterizations of this rate (Demyshev et al. 2012; Kanarska

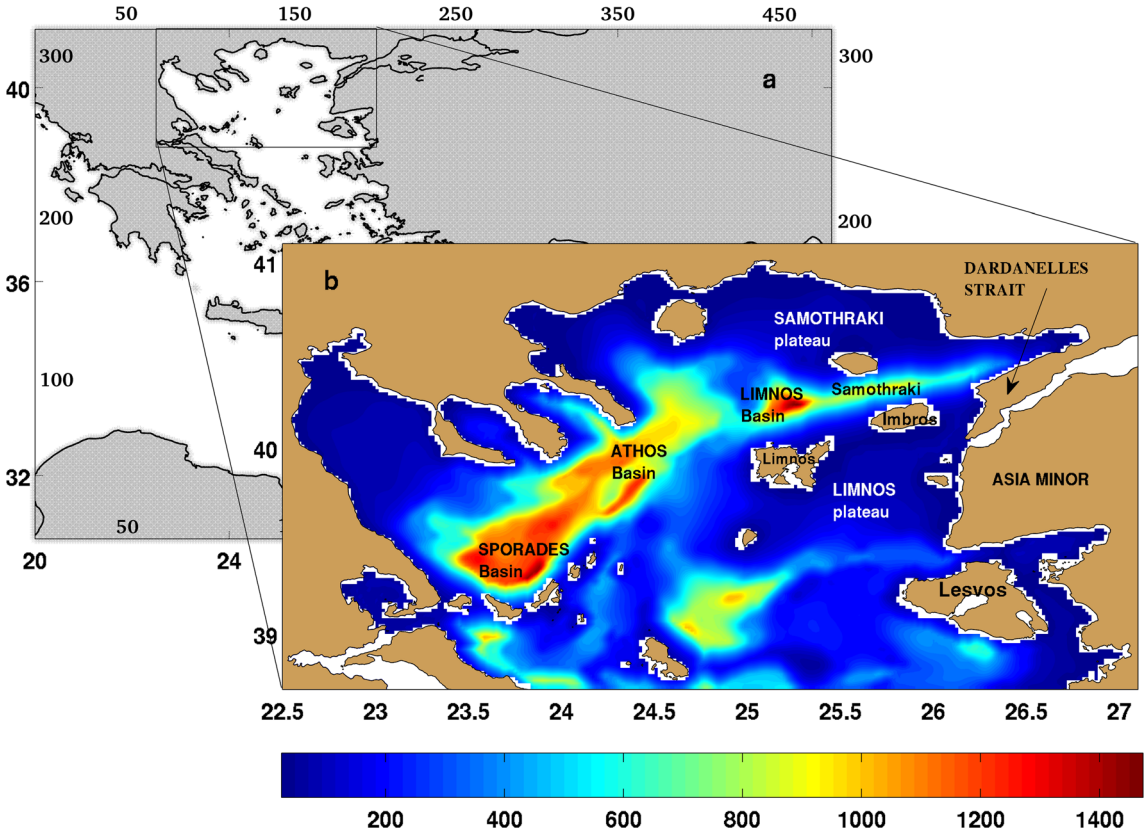

Fig. 1 **a**. Horizontal computational grid points of ALERMO operational system (Eastern Mediterranean). The *box* shows the study area (North Aegean) which is nested in the ALERMO. **b**. Bathymetry map (*m*) of the North Aegean Sea indicating the main basins, islands, and the location of the Dardanelles Strait. The *black solid line* shows a transect used for the presentation of the results

and Maderich 2008; Kourafalou and Barbopoulos 2003; et al. Tuğrul et al. 2002; Tzali et al. 2010; Androulidakis et al. 2012b). However, there are still large uncertainties concerning the variability of inflow/outflow rates on different time scales due to the lack of long-term observational data from the Dardanelles strait. The proposed volume fluxes present different seasonality and amplitude. Although the annual exchange rates differ among the studies (Table 1), most are in agreement in that the net mean annual inflow rate to the North Aegean Sea is about 9.51×10^{-3}Sv.

There are large discrepancies related to the seasonal variability of the BSW inflow rate in the Dardanelles. The seasonality of the flow is related to the seasonal cycle of the riverine freshwater inflow into the Black Sea (Ünlüata et al. 1990), the time it needs to reach the TSS, and the variability of the wind field over the TSS region (Jarosz et al. 2012). The highest river discharge rate usually occurs in spring and is able to change the water budget and convert the Black Sea into a dilution basin (Stanev and Peneva 2002). The signal reaches the TSS two months later (Oğuz and Sur 1989). Thus, the maximum rate of the BSW inflow into the Aegean Sea occurs in summer, and at the same time, the lowest salinity values associated with the BSW are also found in the northeast part of the Aegean Sea (Zodiatis 1994; Beşiktepe et al. 1994; Zervakis et al. 2000). Tuğrul et al. (2002) investigated the seasonal variability of these volume fluxes using

Table 1 Model parameterizations and observational estimations of inflow (towards Aegean), outflow (from the Aegean) and net rates at the Dardanelles Strait (in 10^{-3}Sv)

	Inflow	Outflow	Net
Model parameterizations			
(Zavatarelli and Mellor 1995)	–	–	5.92
(Kourafalou and Barbopoulos 2003)	–	–	9.98
(Nittis et al. 2006)	28.52	19.02	9.50
(Kourafalou and Tsiaras 2007)	20.00	10.00	10.00
(Kanarska and Maderich 2008)	38.81	29.99	8.82
(Demyshev et al. 2012)	26.31	16.80	9.51
Observational estimations			
(Ünlüata et al. 1990)	39.86	30.65	9.51
(Latif et al. 1991)	37.41	27.90	9.51
(Beşiktepe et al. 1994)	38.62	29.10	9.51
(Tuğrul et al. 2002)	42.79	32.47	10.32
(Jarosz et al. 2013)	36.65	31.64	5.01

hydrographic data collected between 1990 and 2000 and Knudsen's approach assuming a steady state mass budget. They have determined that maximum upper- and lower-layer fluxes are observed in spring, while minimum fluxes are in fall. The volume fluxes estimated by Jarosz et al. (2013) based on 14 months of observational data (from August 2008 to October 2009), which are used in this study, present the same seasonality for the BSW inflow (upper-layer fluxes), but the BSW outflow (lower-layer fluxes) is at a maximum in fall and at a minimum in spring. The variability of the Dardanelles inflow is also found to be coherent with the along-strait wind stress and the bottom pressure anomaly gradient (Jarosz et al. 2012).

The Aegean surface circulation shows important spatial and temporal variations. Its complexity is related to the complexity of the coastline and the bottom topography, the inflow of the low-salinity and -temperature BSW and its front with the Levantine waters, the significant river discharge into the basin, and temporal variations of the atmospheric conditions (e.g., the presence of Etesian winds during summer).The basic surface circulation pattern of the BSW inflow from the Dardanelles Strait and its pathways have been discussed in several studies (Zodiatis 1994; Zervakis et al. 2000; Nittis 2003; Tzali et al. 2010).The BSW often bifurcates east of Limnos Island, with the northern branch of the current contributing to a permanent anticyclone around the island of Samothraki (Zervakis and Georgopoulos 2002). At the exit of the Dardanelles Strait, the BSW meets the saltier and warmer waters of Levantine origin (LSW) and a strong salinity front is created. The position of the front fluctuates seasonally around the Island of Limnos as it is located south of Limnos Island during summer and north of the island during winter (Kourafalou and Barbopoulos 2003; Tzali et al. 2010; Androulidakis et al. 2012a).The salinity front moves anticlockwise and its influence is evident up to the Sporades Plateau. All cited studies use different parameterizations of the seasonal exchange fluxes of the BSW inflow. It is also important to evaluate how this circulation pattern is modified by the synoptic-scale pulses of the BSW inflow flux estimates from in situ current observations.

To advance our understanding of the role of the synoptic-scale variability of the BSW inflow on the North Aegean hydrodynamics we conduct a high-resolution numerical simulation of the circulation in the basin using direct observations of the BSW inflow for the period between August 2008 and October 2009 (Jarosz et al. 2013).The objective of this study is to investigate the sensitivity of the North Aegean general circulation and its thermohaline structure to different: (a) time-scale variability (from synoptic to seasonal) of the exchange fluxes and (b) seasonality of the exchange fluxes in the Dardanelles Strait.

The numerical model and its application in the North Aegean Sea are presented in the "Model Configuration" section. The experiments and the simulation results are discussed in the "Results" section. Finally, in the "Discussion and Conclusion" section, findings are summarized and the main conclusions are presented.

2 Model configuration

A numerical model implemented in the North Aegean Sea, is based on the 3-D, primitive-equation, free-surface, and sigma-coordinate Princeton Ocean Model (POM, Blumberg and Mellor 1987). The same model has been used in numerous studies of the general circulation of the Mediterranean Sea and its sub-basins, water mass formation processes, and operational nowcast/forecast systems (Kourafalou and Tsiaras 2007; Skliris et al. 2007; Mantziafou and Lascaratos 2008; Tzali et al. 2010; Vervatis et al. 2013).A time-splitting technique was used in order to estimate the external 2-D (barotropic) and internal 3-D (baroclinic) modes with different time steps. Horizontal diffusivities were calculated according to Smagorinsky (1963), while the vertical mixing coefficients were based on the 2.5 turbulent closure scheme proposed by Mellor and Yamada (1982). The model domain covered the geographical area that lies between 38.7–41.1° N and 22.5–27.1° E. The computational grid had a horizontal resolution of 1/60° × 1/60° and 25 sigma layers in the vertical that were logarithmically distributed near the surface and the bottom in order to correctly represent the dynamics of the Ekman boundary layers. The model bathymetry was from the US Navy Digital Bathymetric Base I (DBDBI) with a resolution of 1/60°. These bathymetric data were interpolated using bilinear interpolation onto the model grid and then smoothed with a third-order Shapiro (1970) smoothing filter.

Initial and open boundary conditions at the southern end of the domain were derived from the operational model ALERMO which provided daily data with a horizontal resolution of 1°/30° × 1°/30° by covering the Aegean and Levantine basins (Sofianos et al. 2006). The ALERMO is one-way nested to the 1°/16° × 1°/16° Mediterranean OGCM model (MyOcean Operational System).

The model used 1-hour atmospheric forcing fields from a high-resolution (1/10°) atmospheric forecasting system SKIRON (Kallos et al. 2005). Atmospheric parameters (wind velocity at 10 m, relative humidity and temperature at 2 m, precipitation, net incoming shortwave radiation, and downward longwave radiation) were used through bulk formulas for the estimation of momentum, heat, and evaporation rates at the air sea interface.

The Dardanelles Strait that controls the exchange between the Black Sea and the Aegean Sea was treated as an open boundary. The flow was imposed as a two-layer system with the inflow of Black Sea waters occupying the upper layer and the outflow of North Aegean Sea waters occupying the lower

layer. The interface was specified at the depth of 13 m as indicated by a zero along-strait velocity crossing (Jarosz et al. 2012). The surface-layer salinity was taken as 28.3 psu (Tzali et al. 2010), whereas the temperature at the boundary was set to that of the adjacent grid point in the interior of the model domain. In the present study, observed upper- and lower-layer volume fluxes of the Dardanelles Strait were used in order to investigate the influence of the BSW synoptic variations.

Fourteen months of observed upper and lower-layer hourly fluxes from the southern Dardanelles Strait are shown in Fig. 2. All the volume fluxes were calculated from measured current velocities. A detailed description of measurements and methodology for volume flux estimations are specified in Jarosz et al. (2013). The hourly data, which were implemented at the open boundary covered the period from 31 August 2009 to 9 October 2009 with gaps between 6 February and 19 February 2009 due to mooring recoveries and subsequent redeployments. The gaps were filled using linear interpolation. The upper-layer volume transport ranged between -62.5×10^{-3}Sv and 85.3×10^{-3}Sv, whereas the lower-layer volume fluxes varied between -53.3×10^{-3}Sv and 78.6×10^{-3}Sv. In the upper-layer, positive values represent a volume flux towards the North Aegean Sea, while in the lower layer; positive values correspond to a volume flux towards the Marmara Sea. In the Aegean section of the Dardanelles Strait the upper-layer currents were impacted by fluctuating wind stress (Jarosz et al. 2012). The annual mean inflow of the BSW into the North Aegean Sea was estimated to be 36.8×10^{-3}Sv and the outflow rate was about 33.6×10^{-3}Sv (RMS error 1.74×10^{-3}Sv and 3.26×10^{-3}Sv, respectively). The variability of the volume fluxes showed different seasonality, when compared with older flux estimations in Dardanelles Strait (Fig. 3). The calculated seasonal cycle showed a maximum value of the upper-layer fluxes during spring 2009(middle May) and a minimum value during fall 2008 (November), while the lower-layer flow was at the maximum during fall 2008 (September) and the minimum during winter 2009 (end of February).The net flow was at the maximum (inflow) during April and the minimum (outflow) at the end of September (Fig. 3a).The different seasonality of exchanges compared with previous studies may be related to the amount of freshwater inflow into the Black Sea for this period (Ünlüata et al. 1990).

The influence of the above-mentioned exchange pattern was compared with a pattern used by Tzali et al. (2010). They employed a parameterization for the exchange rate in Dardanelles Strait, which did not include synoptic time-scale variability. In our parameterization, the annual exchange flow rates estimated by Tuğrul et al. (2002) were used (i.e., 42.79×10^{-3}Sv for the inflow and 32.76×10^{-3}Sv for the outflow). A seasonal cycle was specified by a harmonic equation (Eq. 1), which showed maximum inflow/outflow values in late summer (Fig. 3b).

$$Q_{IN,OUT} = Q_{IN,OUT} + Q_{AMP} \times \cos\left(\frac{2\pi(t_1+t)}{360}\right) \quad (1)$$

Where:

Q_{IN}	0.04279
Q_{OUT}	0.03276
Q_{AMP}	0.015
t	time (days)
t_1	time shift = 120 days

Four experiments (Table 2) were performed for investigating responses of the North Aegean dynamics to different time-scale variability and seasonality of the

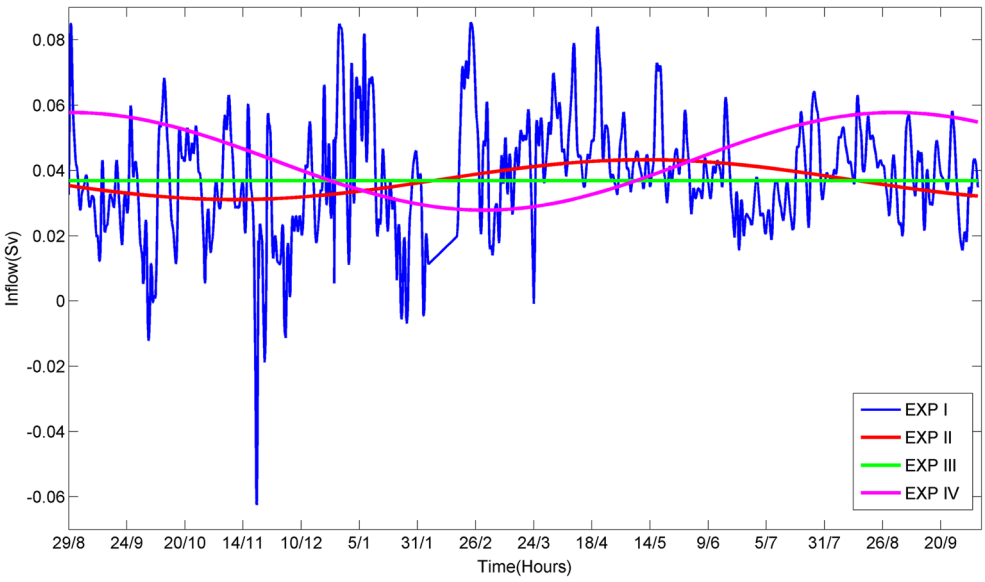

Fig. 2 Observed BSW fluxes (Jarosz et al. 2013) (*blue*: positive values flux towards the Aegean Sea), their seasonal cycle (*red*), mean value calculated from the observed fluxes (*green*), and the parameterization based on Tuğrul et al. 2002 (*magenta*)

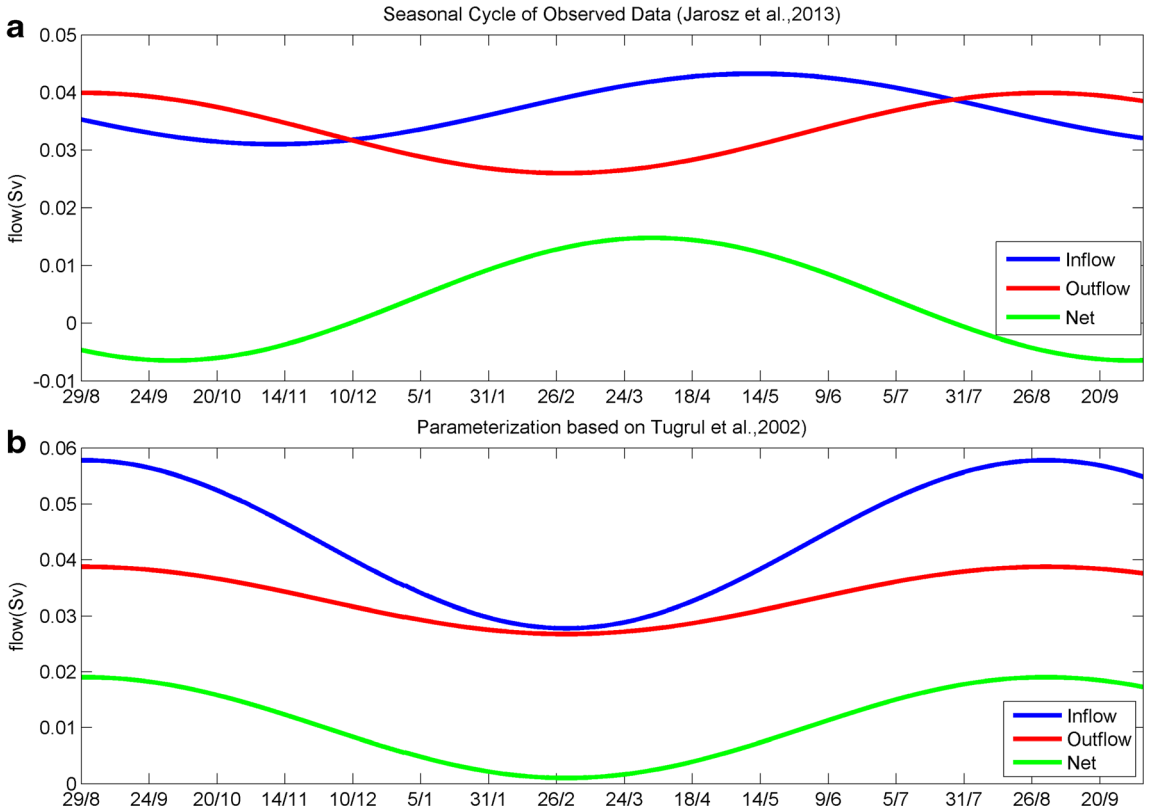

Fig. 3 Annual distribution of Dardanelles inflow (*blue*), outflow (*red*), and net flow (*green*) for observed fluxes (Jarosz et al. 2013) (**a**) and the parameterization based on Tuğrul et al. 2002 (**b**)

exchange rates in the Dardanelles Strait. The first three experiments investigated the response of the North Aegean basin to the observed volume fluxes (Jarosz et al. 2013). The first experiment (EXP I) used the original exchange volume rates between the Black Sea and the North Aegean Sea, which included the synoptic variations of the flow. In EXP II, the seasonal cycle of the observed inflow/outflows were used, whereas in EXP III, a constant inflow/outflow rates which were the averages of the seasonal cycle of EXP II (37.8×10^{-3}Sv for the inflow and 32.8×10^{-3}Sv for the outflow) were applied. The parameterization of annual exchange rates of the Dardanelles flow based on Tuğrul et al. (2002) was implemented in EXP IV to evaluate effects of the different seasonal variability of the exchange flow on flow dynamics in the North Aegean.

Table 2 List of experiments

Inflow/outflow	
Experiment I	Observed Dardanelles fluxes (Jarosz et al. 2013)
Experiment II	Seasonal cycle of observed data
Experiment III	Constant mean value of observed data
Experiment IV	Parameterization based on Tuğrul et al. 2002

3 Results

3.1 Spatial distribution of thermohaline features

The spatial distribution of the near-surface salinity (Fig. 4) constitutes the best parameter for investigating the influence of BSW and its variability on the North Aegean dynamics. The mean surface salinity and circulation patterns (Figs. 4 and 5) for all experiments are very similar although there are important smaller scale differences that will be discussed later on. All main features of the large-scale salinity distribution and circulation of the North Aegean persist. There is a marked difference in salinity between the southern and northern parts of the domain. Higher salinity associated with the waters of Levantine origin dominates in the south and lower salinity associated with the effect of the BSW inflow covers the northern part. The brackish water exits the Dardanelles Strait as a strong density current that is deflected to the north and passes between the Imvros and Samothraki Islands. Then it shifts southwestwards reaching the Sporades plateau with much higher velocities compared to the mean basin current field. The absence of seasonal variability of the BSW inflow rate (EXP III) results in a more intense circulation with enhanced mesoscale activity (Fig. 5). In this experiment, the volume fluxes during winter are increased (compared to the experiment including the seasonal variability) and thus the presence

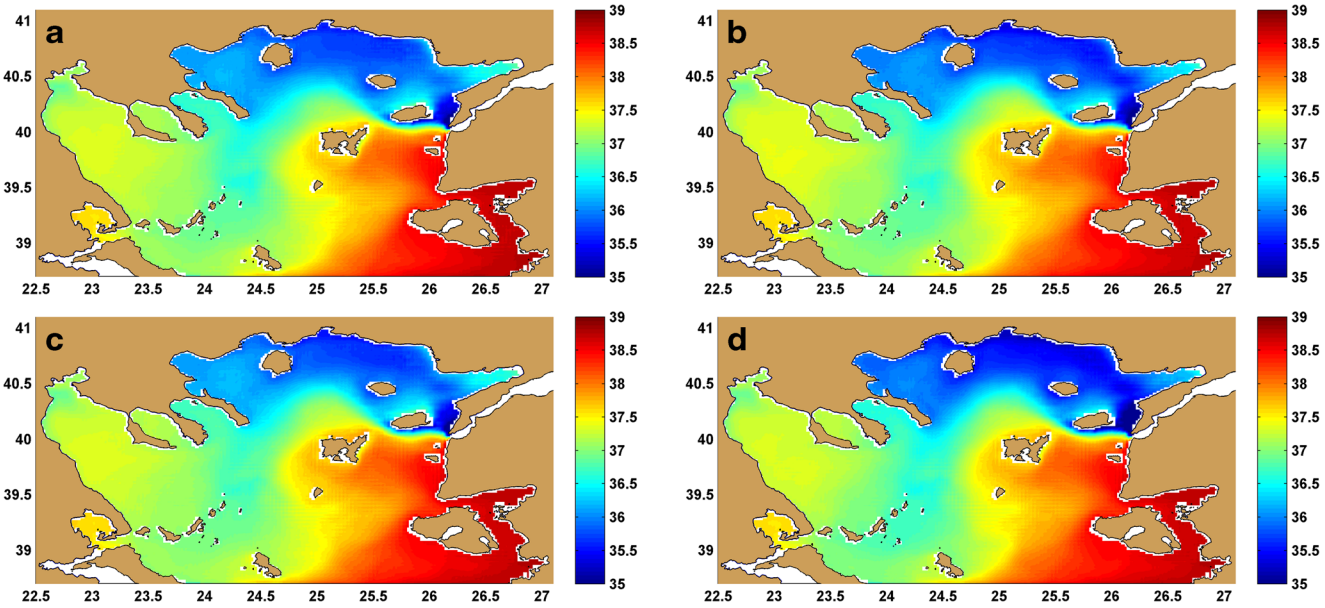

Fig. 4 Mean annual salinity field at 10 m for experiment I (**a**), experiment II (**b**), experiment III (**c**), and experiment IV (**d**)

of a constant and higher exchange flow leads to greater density gradients. In this case the influence of the BSW is more intense in driving the surface circulation and maintaining anti-cyclonic and cyclonic structures in the basin. Also the different seasonality (EXP IV) and the higher inflow seem to block the low-salinity BSW in the northeastern part of the basin showing lower salinity than in EXPI II, and III in this area. The lower net flow in EXP II than in EXP IV also leads to a weaker surface circulation (Fig. 5b and d)

Comparing experiments I, II, and IV during winter (Fig. 6a, c, and e) the decreased BSW inflow, combined with the intense evaporation that dominates in the North Aegean during this season, induces a higher salinity than in summer (Fig. 6b, d, f), when lower salinity water masses cover the larger part of the basin and displace the surface waters of Levantine origin (LSW) southeastward. Thus, during summer the BSW/LSW front is located farther south (south of Imvros and Limnos islands) than in winter (north of Imvros and Lemnos Islands) as it is also reported by previous works (Androulidakis et al. 2012a; Kourafalou and Barbopoulos 2003; Tzali et al. 2010). The velocity in the basin is enhanced in summer and the circulation is stronger as the BSW flow has

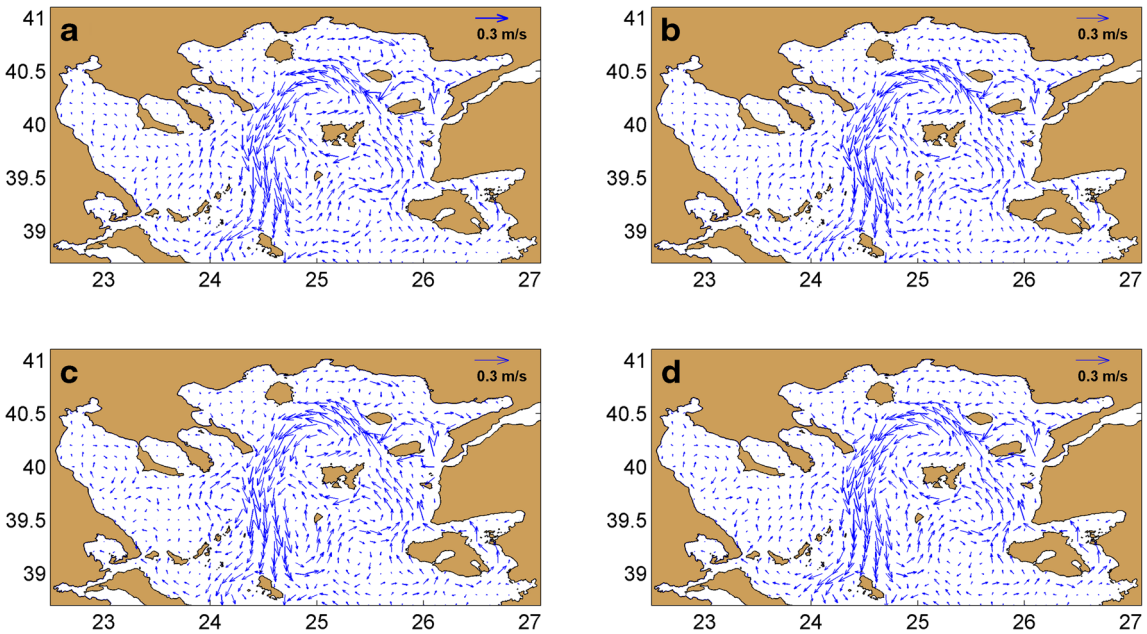

Fig. 5 Mean annual current velocity field (m/s) at 10 m for: experiment I (**a**), experiment II (**b**), experiment III (**c**), and experiment IV (**d**)

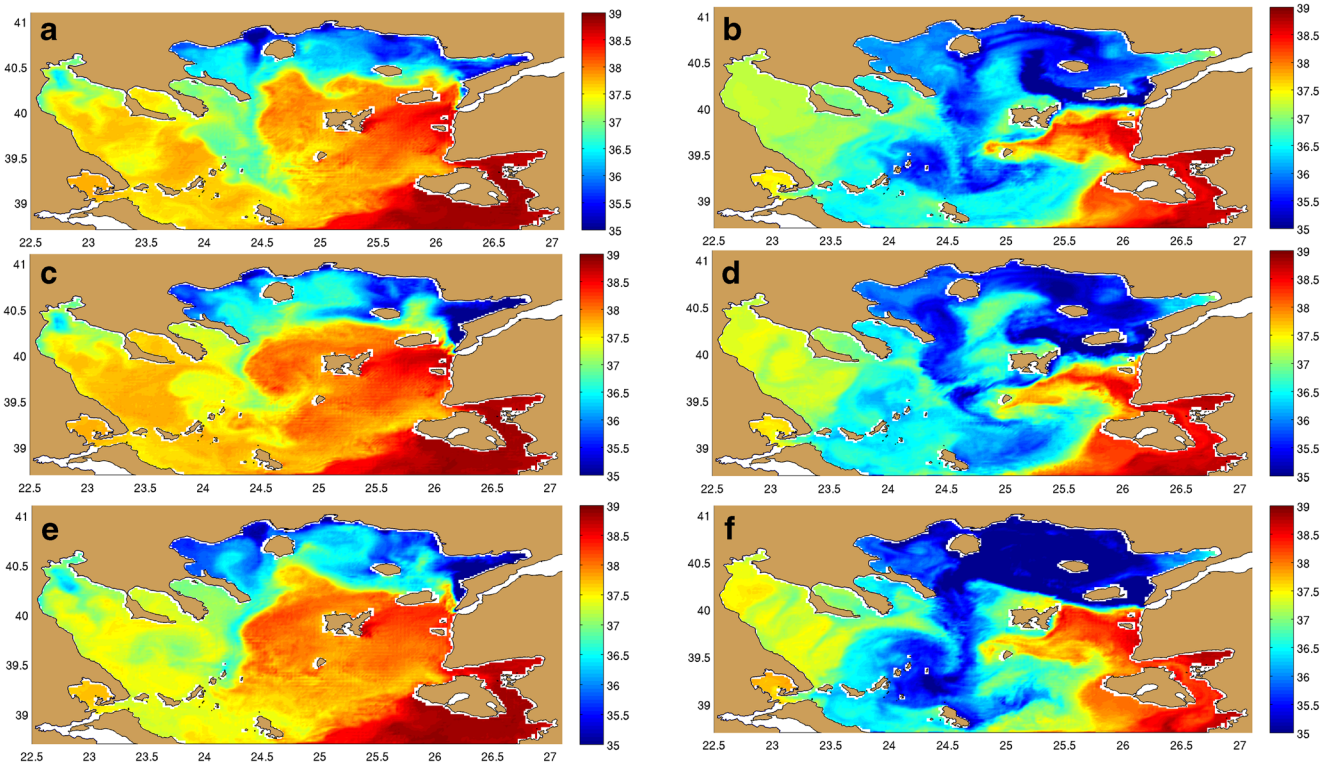

Fig. 6 Mean salinity field at 10 m in February (**a**, **c,** and **e**), August (**b**, **d**, and **f**) for experiment I (**a** and **b**), experiment II (**c** and **d**), and experiment IV (**e** and **f**), respectively

the maximum values and large amount of brackish water spreads inside the basin. (Fig. 7b, d, f).During winter in EXPI, the front between the BSW and LSW is more unstable than in EXPII and shows a meandering pattern probably due to including synoptic variations in the BSW fluxes in EXPI. In EXPIV, the BSW influences the salinity of the western basin,

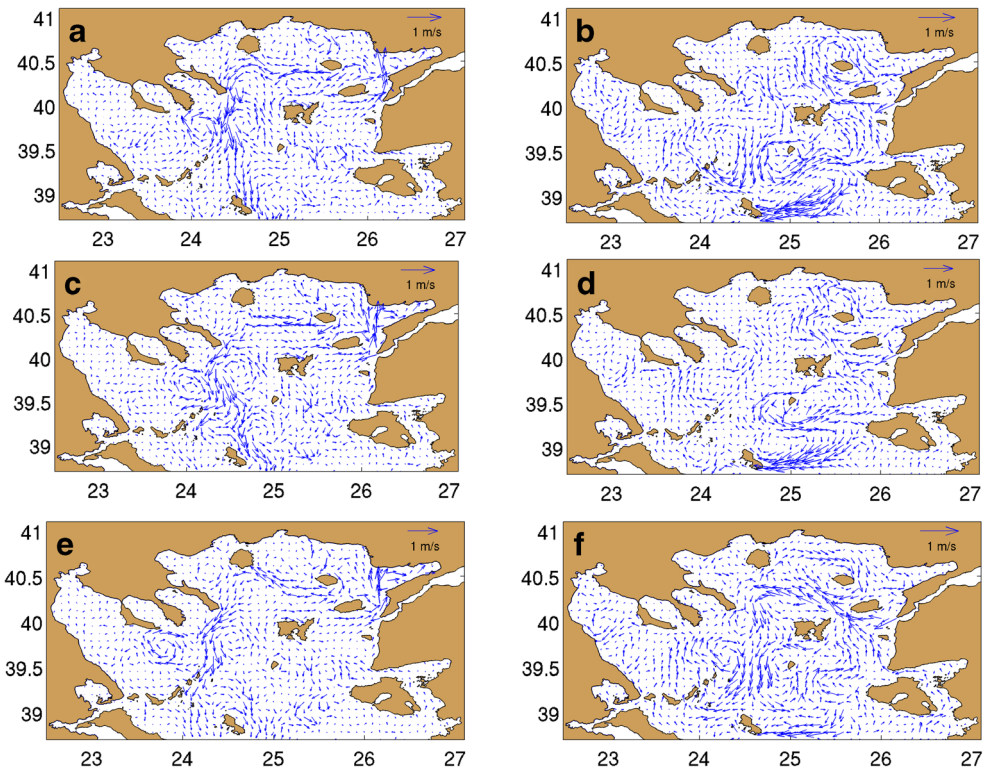

Fig. 7 Experiment I: mean velocity field (m/s) at 10 m in February (**a**, **c,** and **e**), August (**b**, **d,** and **f**) for experiment I (**a** and **b**), experiment II (**c** and **d**), and experiment IV (**e** and **f**), respectively

which is lower than in EXPI and EXPII, especially during winter. Larger salinity gradient between the BSW and LSW is obvious in EXPIV during summer, when the BSW flux is maximal.

3.2 Temporal variability of hydrographic characteristics

Although the influence of the inflowing BSW is mainly confined to the surface layer, the entire water column of the basin is eventually affected. The annual mean basin-averaged salinity of the North Aegean Sea is shown in Fig. 8a. The seasonal cycle is evident for all experiments with maximum salinity values during winter, when the BSW inflow is the lowest. A reduction in salinity throughout the spring and minimum values at the end of summer is related with the maximum BSW spreading in the basin. Differences among the experiments resulting from the amplitude and the seasonal-cycle phase are observed. The seasonal cycle of the basin-averaged salinity (Fig. 8b) in EXP I and EXP II has a similar range with a phase lag of about 1 month in summer 2009. The salinity minimum in EXP I and EXP II is observed about 2–3 months after the maximum BSW inflow as reflected by the basin-averaged salinity. The maximum salinity in EXP I, EXP II, and EXP IV shows a time shift, which may play an important role in the deep water formation processes in the region. The salinity maximum in EXP I occurs in late January, a few days earlier than in EXP II, while the maximum salinity in EXP IV is in the middle of March. The inflow and outflow rates of the parameterized fluxes (EXP IV) are in phase, but the observed data (EXPII) show that there is a phase lag of about 3.5 months, and the net flow impacts the volume integrated salinity. The salinity minimum arrives about 2 months later than the BSW maximum net flow. The net flow in EXP II is smaller than in EXP IV and becomes negative (net flow towards the Marmara Sea), and thus minimum values of salinity occur later in EXP II than in EXP IV (~4 months). The use of parameterization based on Tuğrul et al. 2002 for the exchange rate in the Dardanelles Strait results in lower mean salinity of the water column, as the net rate of flow towards the Aegean Sea is higher in EXP IV compared to the rate in EXP II (i.e., 10.32×10^{-3}Sv and 5.01×10^{-3}Sv, respectively).The same pattern is more pronounced in the upper part of the water column (0–10 m) (Fig. 9) as saltier and thus denser water appears earlier in winter (EXP I and EXP II) at the surface and thus, the vertical mixing could be facilitated, enhanced by the strong local winds and high negative net heat flux. The basin-averaged kinetic energy for all experiments (Fig. 10) is minimum at the end of spring and maximum during winter mainly following the seasonality of the

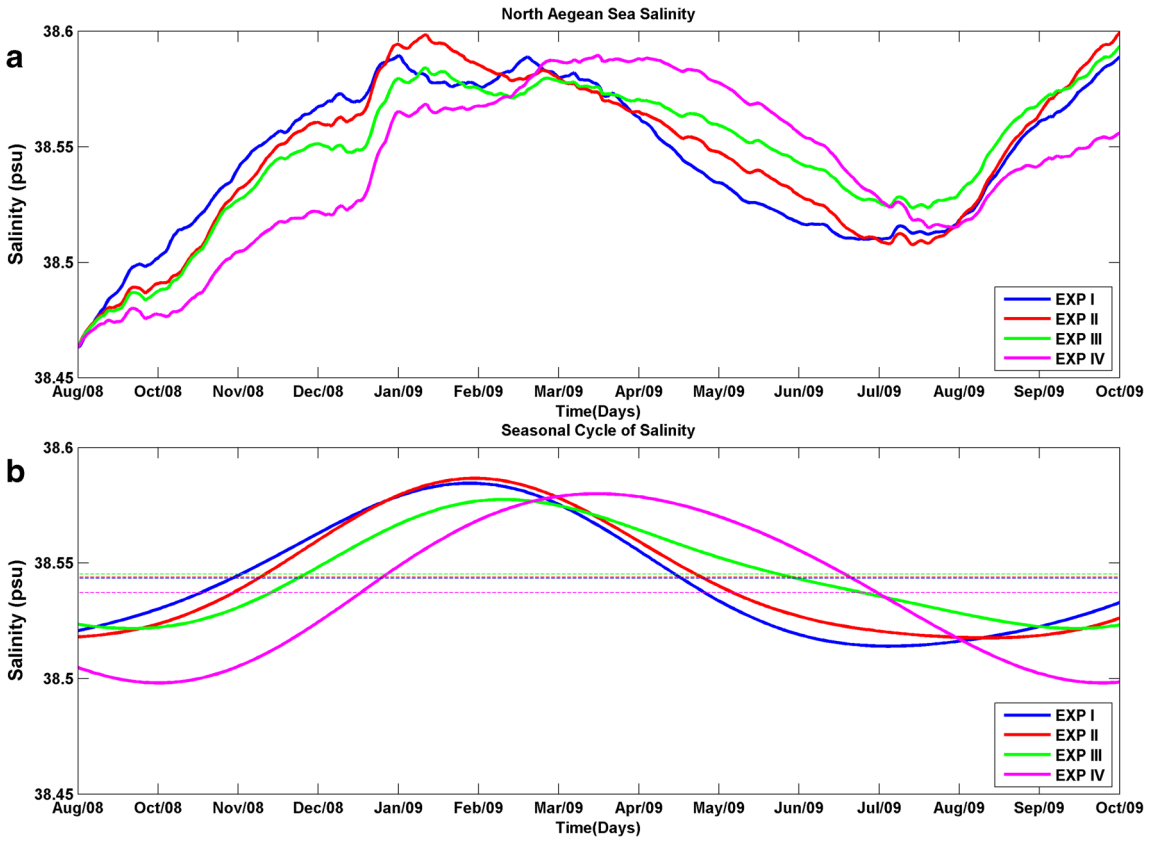

Fig. 8 Daily values of basin-averaged salinity (**a**), and seasonal cycle of basin-averaged salinity (**b**)

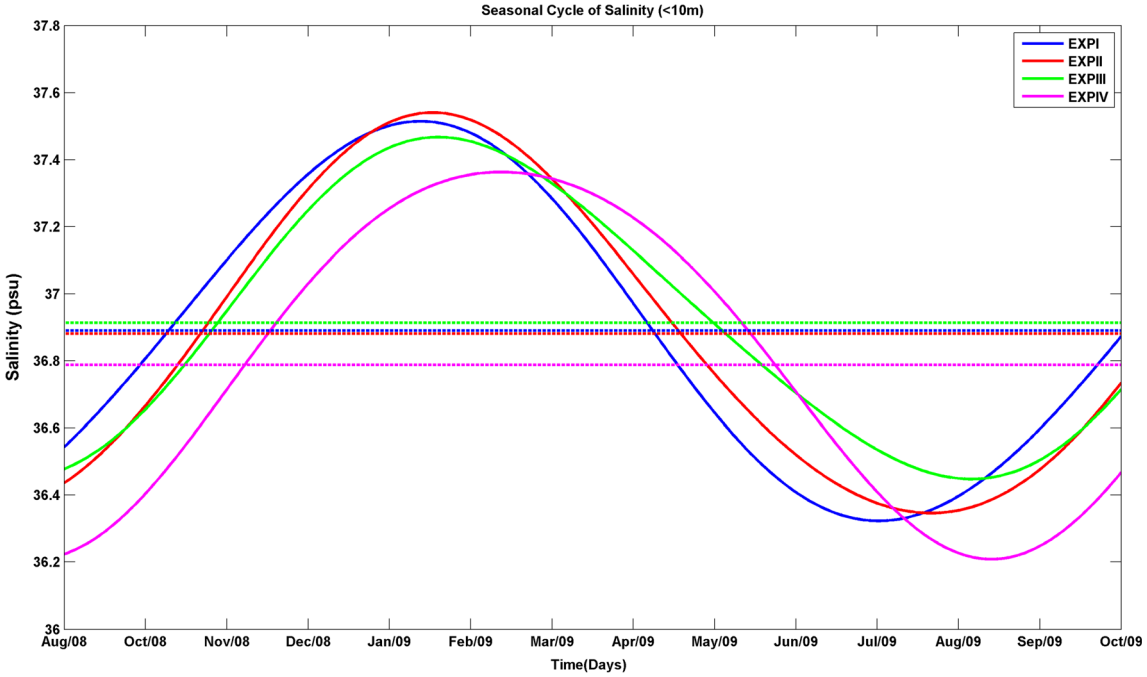

Fig. 9 Seasonal cycle of basin-averaged salinity for depths between 0 and 10 m for all experiments

local winds. Tzali et al. (2010) have concluded that the accumulation of efficient quantities of brackish water can lead to large density gradients and strong currents contributing to the increase of the basin kinetic energy. In EXP I, the BSW flow in the North Aegean is intermittent and this disrupts the steady accumulation of the BSW in the circulation features making them weaker and decreasing the overall kinetic energy in the North Aegean basin.

3.3 The role of the synoptic time-scale variations of BSW inflow

The impact of the synoptic time-scale variability of the volume fluxes can be easily identified by comparing EXP I and EXP II. EXP II has the same mean fluxes and the same seasonal cycle, but lacks the synoptic variability in the inflow and outflow rates. As shown above, the basin-average kinetic energy of EXP II (after removing the synoptic variability) is

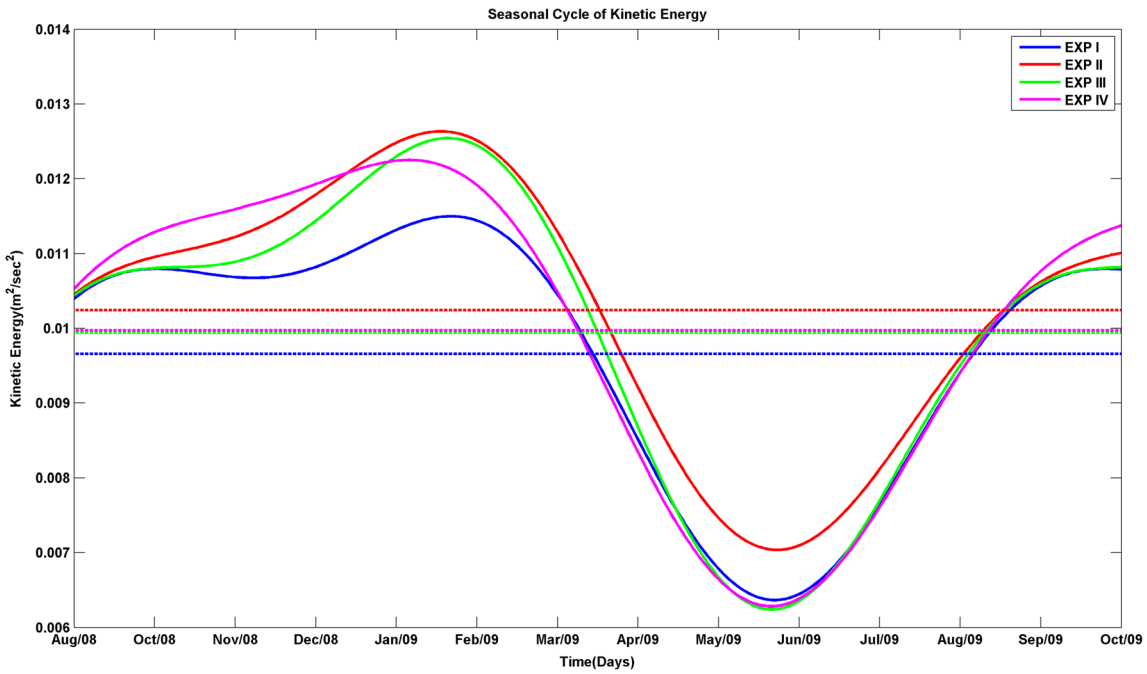

Fig. 10 Seasonal cycle of basin-averaged kinetic energy for all experiments

considerably increased, compared to the inflow with synoptic time-scale variations included in EXP I. The presence of a steady seasonal inflow (EXP II) enhances the along-front current, which is located north of Limnos, and creates strong structures and cyclonic eddies (Fig. 11a). The existence of synoptic time-scale variations in the BSW inflow does not allow the circulation of the basin to develop completely and also restricts the accumulation of low-salinity waters. As shown in Fig. 2, the brackish water mass in the upper layer sometimes flows towards the Aegean Sea and some others towards the Marmara Sea as shown by sharp pulses. As a result, the high-frequency variations of the BSW inflow inhibit the development of several structures and reduce the kinetic energy of the basin. In contrast, the presence of a steady seasonal inflow intensifies features associated with the BSW circulation and leads to higher kinetic energy at the surface. Furthermore, the stronger circulation pattern in the inflow area induces the enhancement of the water mass exchanges at the southern open boundary that leads to a northward displacement of the front between the BSW and the high-salinity waters of Levantine origin. Larger amounts of the high-salinity LSW are then present in area north of the Lesvos Island and thus the salinity of the basin increases. The maximum salinity differences between EXP I and EXP II in this area reach 0.31 psu. The main path of BSW inflow in EXP II is displaced to the northwest of the Limnos Island as indicated by differences in the kinetic energy distribution between the two experiments, which show 0.0053 m^2/s^2 higher kinetic energy than EXP I in the area north of Lemnos. (Fig. 11b). A patch of higher salinity water is observed in the region north of Limnos, following the displacement of the front, permitting an inflow of Levantine waters into the Limnos-Lesvos plateau (Fig. 11c). The displacement of the front between the two experiments is also obvious in the temperature field (Fig. 11d). Comparison of the surface salinity fields between EXP I and EXP III as well as between EXPI and EXP IV (Fig. 11e, f) show that different seasonality of the low-salinity inflow leads to more intense salinity differences all along the basin. The influence of a constant inflow rate on the salinity spatial distribution has been also discussed by Tzali et al. (2010).

As the region north of the island of Lemnos plays an important role on dense water formation processes (Zervakis et al. 2000), a further investigation about the vertical structure in this area has been conducted. A vertical cross-section along 40.18° N (Fig. 1) depicts salinity and density distribution through the Lemnos Plateau in February for EXP I and EXP II (Fig. 12). In EXP I the salinity and the σ_θ of the upper layer are decreased to about 0.73 psu and 0.56 kg m^{-3}, respectively. The northern displacement of the salinity front in EXPII as a result of the higher kinetic energy in EXP II results in weaker stratification in the area north of Lemnos in comparison to

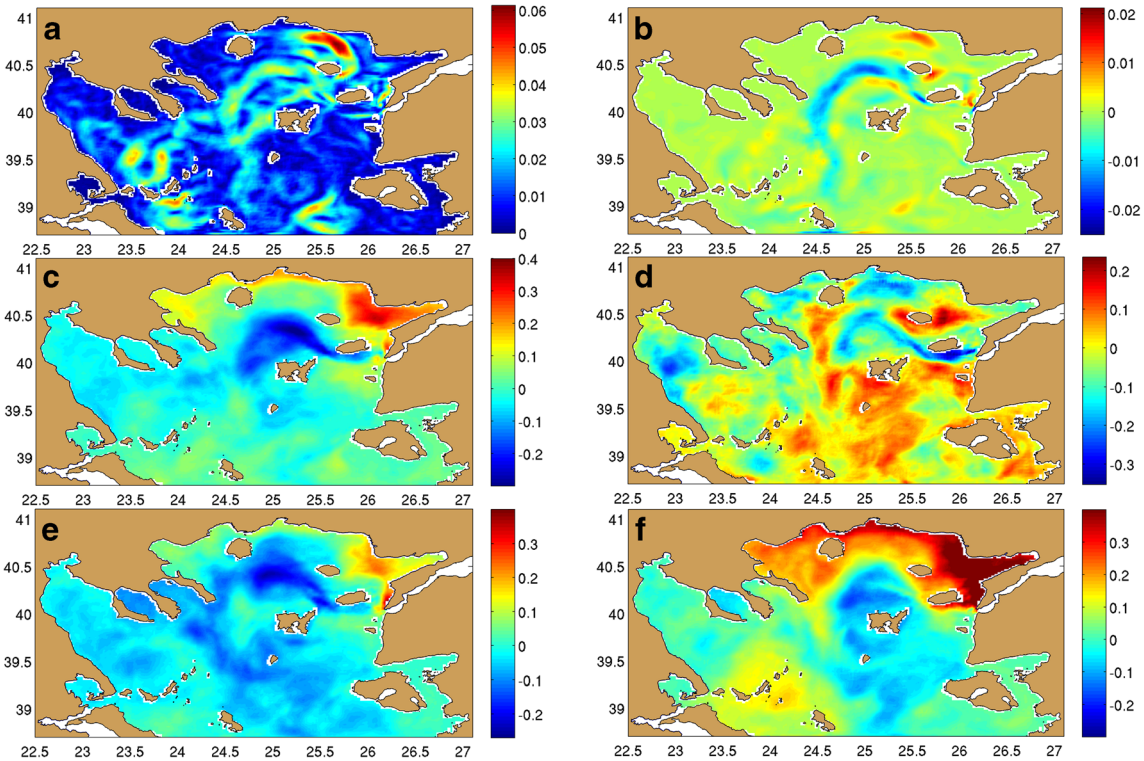

Fig. 11 Difference at 10 m between EXP I and EXP II for the mean velocity field (m/s) (**a**), the kinetic energy of the mean flow (m^2/s^2) (**b**), the mean salinity field (psu) (**c**) and the mean temperature field (°C) (**d**), EXP I–EXP III mean salinity (**e**), and EXP I–EXP IV mean salinity (**f**) (all mean fields are for the whole period)

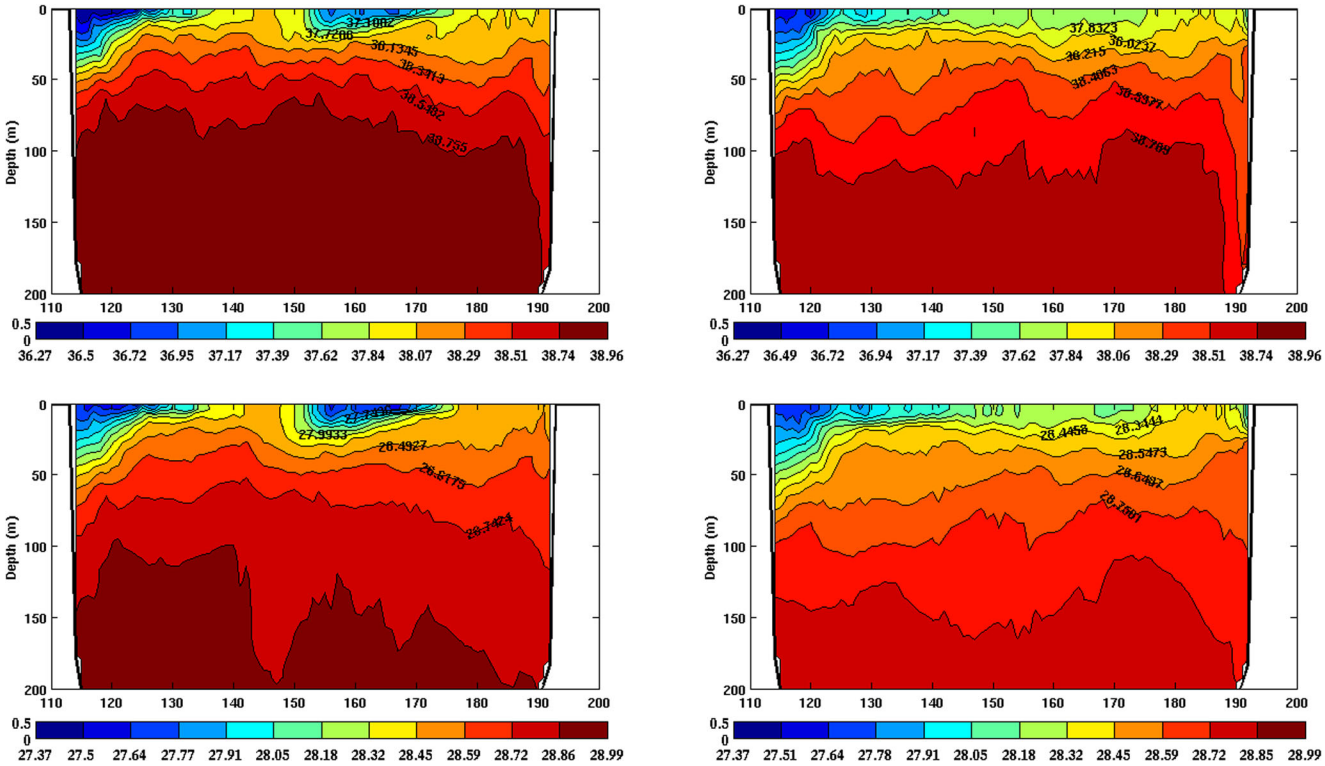

Fig. 12 Vertical section of salinity and σ_θ along 40.18° N in February (monthly mean) between 24.31–25.81° E for EXP I (*left*) and EXP II (*right*)

EXPI. The higher kinetic energy in EXP II leads to larger vertical exchanges and results to a weaker water stratification. In the contrary, the insertion of synoptic variations preserves lower salinity waters in this area resulting to a stronger stratification. Thus, the variations of the BSW inflow could change the salinity distribution in the North Aegean as discussed by previous studies (Stanev and Peneva 2002).

4 Discussion and conclusions

In this work the role of the synoptic time-scale variations of the Black Sea Water inflow to the Aegean over the period from August 2008 to October 2009 is investigated. A high-resolution ocean model was applied to the area of the North Aegean, using upper and lower-layer fluxes estimated from current observations collected in the Dardanelles Strait (open boundary). Four sensitivity experiments were carried out in order to identify the mechanisms related to the response of the North Aegean to the BSW fluxes and their synoptic and seasonal variations.

The basin-scale surface circulation pattern of the North Aegean is not significantly altered in the various experiments, showing that the main structures are maintained. However, the seasonality of the BSW inflow significantly affected the salinity content of the water column on a seasonal time-scale. The implementation of the observed inflow rates led to the earlier appearance of the maximum values of the basin salinity, which may play an important role in the deep water formation processes. The use of parameterization based on flux values estimated by Tuğrul et al.(2002) for the BSW inflow resulted in lower basin-averaged salinity, as the net flux of this parameterization was 50 % higher than that estimated from the observations. The exchange flow rates of the BSW towards the North Aegean are a significant factor affecting the circulation in the basin. The presence of synoptic time-scale variations in the BSW inflow led to lower basin-averaged kinetic energy, as the synoptic time-scale pulses of inflow/outflow from the Dardanelles Strait resulted in a weaker circulation pattern and inhibited the development of several circulation structures in the area. The presence of steady seasonal inflow enhanced the circulation in the basin and thus the exchanges with the Southern Aegean. A northward displacement of the front between the BSW and the high-salinity waters of Levantine origin is also evident and higher salinity water is observed north of Limnos.

The displacement of the front also affects the vertical column structure in the area north of Lemnos, which is considered as a dense water mass formation area. High-frequency variations at the Dardanelles strait exchanges lead to stronger stratification in this area.

The results of this study offer new insights into the ways that the higher frequency variability of the exchange fluxes from the Dardanelles Strait can affect the thermohaline circulation and vertical structure in the North Aegean. Proper representation of the Dardanelles exchanges is very crucial for

improvements of the operational systems of the Eastern Mediterranean. Better understanding of the dynamics of the North Aegean requires longer time series of observational data to improve the open boundary conditions in the Dardanelles Strait.

References

Androulidakis YS, Kourafalou VH, Krestenitis YN, Zervakis V (2012a) Variability of deep water mass characteristics in the North Aegean Sea: the role of lateral inputs and atmospheric conditions. Deep Res Part I Oceanogr Res Pap 67:55–72. doi:10.1016/j.dsr.2012.05.004

Androulidakis YS, Krestenitis YN, Kourafalou VH (2012b) Connectivity of the North Aegean circulation to the Black Sea water budget. Cont Self Res 48:8–26. doi:10.1016/j.csr.2012.08.019

Beşiktepe ŞT, Sur Hİ, Özsoy E et al (1994) The circulation and hydrography of the Marmara Sea. Prog Oceanogr 34:285–334. doi:10.1016/0079-6611(94)90018-3

Blumberg A, Mellor G (1987) A description of a three-dimensional coastal ocean circulation model. Coast Estuar Sci 1–16

Demyshev SG, Dovgaya SV, Ivanov VA (2012) Numerical modeling of the influence of exchange through the Bosporus and Dardanelles Straits on the hydrophysical fields of the Marmara Sea. Izv Atmos Ocean Phys 48:418–426. doi:10.1134/S0001433812040056

Jarosz E, Teague WJ, Book JW, Beşiktepe ŞT (2012) Observations on the characteristics of the exchange flow in the Dardanelles Strait. J Geophys Res 117:C11012. doi:10.1029/2012JC008348

Jarosz E, Teague WJ, Book JW, Beşiktepe ŞT (2013) Observed volume fluxes and mixing in the Dardanelles Strait. J Geophys Res Ocean 118:5007–5021. doi:10.1002/jgrc.20396

Kallos G, Sofianos S, Pytharoulis I. KP and SN (2005) Limited area atmosphere/ocean forecasting system for the East Mediterranean MFSTEP activities: performance analysis

Kanarska Y, Maderich V (2008) Modelling of seasonal exchange flows through the Dardanelles Strait. Estuar Coast Shelf Sci 79:449–458. doi:10.1016/j.ecss.2008.04.019

Kourafalou VH, Barbopoulos K (2003) High resolution simulations on the North Aegean Sea seasonal circulation. Ann Geophys 21:251–265

Kourafalou V, Tsiaras K (2007) A nested circulation model for the North Aegean Sea. Ocean Sci 3:1–16. doi:10.5194/os-3-1-2007

Latif MA, Özsoy E, Oguz T, Ünlüata Ü (1991) Observations of the Mediterranean inflow into the Black Sea. Deep Sea Res Part A Oceanogr Res Pap 38:S711–S723. doi:10.1016/S0198-0149(10)80005-6

Mantziafou A, Lascaratos A (2008) Deep-water formation in the Adriatic Sea: interannual simulations for the years 1979–1999. Deep Sea Res Part I Oceanogr Res Pap 55:1403–1427. doi:10.1016/j.dsr.2008.06.005

Mellor G, Yamada T (1982) Development of a turbulence closure model for geophysical fluid problems. Rev Geophys 20:851. doi:10.1029/RG020i004p00851

Nittis K (2003) Dense water formation in the Aegean Sea: numerical simulations during the Eastern Mediterranean Transient. J Geophys Res 108:8120

Nittis K, Perivoliotis L, Korees G, et al (2006) Operational monitoring and forecasting for marine environmental applications in the Aegean Sea. Environ Model Softw 21:243-257. doi:10.1016/j.envsoft.2004.04.023

Oğuz T, Sur IH (1989) A 2-layer model of water exchange through the Dardanelles strait. Oceanol Acta 12(1):23–31

Shapiro R (1970) Smoothing, filtering, and boundary effects. Rev Geophys 8:359–387

Skliris N, Sofianos S, Lascaratos A (2007) Hydrological changes in the Mediterranean Sea in relation to changes in the freshwater budget: a numerical modelling study. J Mar Syst 65:400–416. doi:10.1016/j.jmarsys.2006.01.015

Smagorinsky J (1963) General circulation experiments with the primitive equations. Mon Weather Rev 91:99–164. doi:10.1126/science.27.693.594

Sofianos SS, Skliris N, Mantziafou A et al (2006) Nesting operational forecasting models in the Eastern Mediterranean: active and slave mode. Ocean Sci Discuss 3:1225–1254. doi:10.5194/osd-3-1225-2006

Stanev EV, Peneva EL (2002) Regional sea level response to global climatic change: Black Sea examples. Glob Planet Chang 32:33–47

Tuğrul S, Beşiktepe S, Salihoglu I (2002) Nutrient exchange fluxes between the Aegean and Black Seas through the Marmara Sea. Mediterr Mar Sci 3:33–42. doi:10.12681/mms.256

Tzali M, Sofianos S, Mantziafou A, Skliris N (2010) Modelling the impact of Black Sea water inflow on the North Aegean Sea hydrodynamics. Ocean Dyn 60:585–596. doi:10.1007/s10236-010-0277-3

Ünlüata Ü, Oguz T, Latif MA, Ozsoy E (1990) On the physical oceanography of the Turkish Straits. Phys Oceanogr Sea Straits, Ed by L J Pratt, 25–60. doi: 10.1007/978-94-009-0677-8

Vervatis VD, Sofianos SS, Skliris N et al (2013) Mechanisms controlling the thermohaline circulation pattern variability in the Aegean–Levantine region. A hindcast simulation (1960–2000) with an eddy resolving model. Deep Sea Res Part I Oceanogr Res Pap 74:82–97. doi:10.1016/j.dsr.2012.12.011

Zavatarelli M, Mellor GL (1995) A numerical study of the Mediterranean Sea circulation. J Phys Oceanogr 25:1384–1414

Zervakis V, Georgopoulos D (2002) Hydrology and circulation in the North Aegean (eastern Mediterranean) throughout 1997 and 1998. Mediterr Mar Sci 3:5–19. doi:10.12681/mms.254

Zervakis V, Georgopoulos D, Drakopoulos PG (2000) The role of the North Aegean in triggering the recent Eastern Mediterranean climatic changes. J Geophys Res 105:26103. doi:10.1029/2000JC900131

Zodiatis G (1994) Advection of the Black Sea water in the North Aegean Sea. Glob Atmos Ocean Syst 2:41–60